

Nanoscale α -structural domains in the phonon-glass thermoelectric material β -Zn₄Sb₃H. J. Kim,¹ E. S. Božin,¹ S. M. Haile,² G. J. Snyder,² and S. J. L. Billinge^{1,*}¹Department of Physics and Astronomy, Michigan State University, East Lansing, Michigan 48824-1116, USA²Department of Materials Science, California Institute of Technology, Pasadena, California 91125, USA

(Received 8 January 2007; published 18 April 2007)

A study of the local atomic structure of the promising thermoelectric material β -Zn₄Sb₃, using atomic pair distribution function (PDF) analysis of x-ray- and neutron-diffraction data, suggests that the material is nanostructured. The local structure of the β phase closely resembles that of the low-temperature α phase. The α structure contains ordered zinc interstitial atoms which are not long range ordered in the β phase. A rough estimate of the domain size from a visual inspection of the PDF is $\lesssim 10$ nm. It is probable that the nanoscale domains found in this study play an important role in the exceptionally low thermal conductivity of β -Zn₄Sb₃.

DOI: 10.1103/PhysRevB.75.134103

PACS number(s): 72.20.Pa, 61.10.Nz, 61.12.Ld, 73.50.Lw

Thermoelectric materials allow for direct conversion of heat into electrical energy and vice versa. They hold great technological promise for solid-state refrigeration and power generation¹ if the dimensionless figure of merit, ZT , can be pushed above 2. The materials' challenge is to minimize thermal conductivity without reducing the electrical conductivity, i.e., to produce strong scattering of phonons, but not electrons. The simple and nominally stoichiometric β -Zn₄Sb₃ (Ref. 2) is an excellent example of such a phonon-glass³ thermoelectric material and presents a model system for studying this phenomenon, but the mechanism for the low thermal conductivity is not established.^{2,4-6} Here, we show that interstitial Zn atoms^{2,5} not only provide point defects but also force a local structural rearrangement on the nanometer scale in β -Zn₄Sb₃. These nanodomains should effectively scatter the long wavelength phonons that are important for heat transport.⁷⁻¹⁰ This strongly supports the view that nanoscale structural modulations are an important ubiquitous component in emerging high ZT materials.⁷⁻¹²

The $ZT = S^2 \sigma T / \kappa$, where S , σ , and κ are the Seebeck coefficient, electrical conductivity, and thermal conductivity, respectively, of β -Zn₄Sb₃ exceeds unity above 540 K.² It crystallizes in space group $R\bar{3}c$ (Fig. 1). Several different structural defects have been proposed to exist in the lattice such as Zn and Sb mixed sites¹³ and an occupational deficiency on Zn sites.⁴ The recent proposal of interstitial Zn atom defects in the crystal structure of β -Zn₄Sb₃ (Refs. 2 and 5) would increase phonon scattering and therefore ZT . However, such point defects are expected to scatter short-wavelength phonon more effectively than mid- to long-wavelength phonons,^{7,10} the major agents of heat conduction in alloys.⁷ The point defects alone are unlikely to explain the exceptionally low thermal conductivity. We used the atomic pair distribution function (PDF) analysis^{14,15} of x-ray and neutron scattering data to study the local structure in β -Zn₄Sb₃. The PDF method, a local structural probe that yields the probability of finding an atom at a distance r away from another atom, has been successfully applied to solve the structures of disordered crystals.¹⁵ The high-symmetry rhombohedral structure and nominally stoichiometric composition of β -Zn₄Sb₃ hides an interesting underlying complexity that is revealed by these local structural measurements. By comparing the experimental PDF of Zn₄Sb₃ with

PDFs calculated from several structural models, we show that, locally, the material retains its low-symmetry low-temperature form^{16,17} and the higher-symmetry average structure is due to averaging of these nanometer scale local domains. Temperature-dependent measurements through the α - β transition support this picture. We have estimated the domain size at less than 10 nm from a comparison of low- and high-temperature PDFs determined over a wide range of r . Interestingly, the length scale of this intrinsically self-organized nanodomains observed in the high ZT β form of the material is comparable to the length scale of nanoscale superstructures^{11,12} or defects⁷⁻¹⁰ introduced in newly engineered high ZT materials to efficiently scatter mid-to long-wavelength phonons. This is a report on nanoscale domains in β -Zn₄Sb₃, and the compelling similarity in the order of domains size to nanoscale structural modulations in other high ZT materials strongly suggests their important role in very low thermal conductivity of β -Zn₄Sb₃.⁷

Two Zn₄Sb₃ samples (I and II) were prepared at different times by direct reaction of the elements. Neutron-powder diffraction measurements were carried out on sample I at 15 and 300 K using the NPDF diffractometer at the Lujan Center at Los Alamos National Laboratory. X-ray powder-diffraction data for sample II were collected at room temperature and over a range of temperatures to 150 K at the 6-IDD station at the Advanced Photon Source at Argonne National Laboratory. The x-ray energies were 87.006 keV

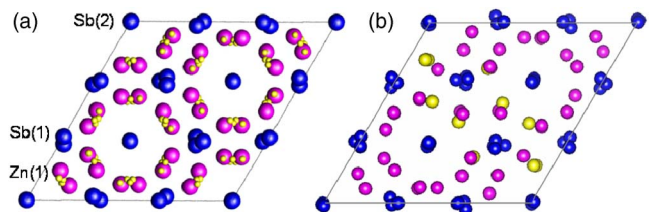


FIG. 1. (Color online) The crystal structure of Zn₄Sb₃. (a) Projection down the c axis of the crystal structure of β -Zn₄Sb₃ in space group $R\bar{3}c$. There are three distinct atomic positions, 36Zn(1), 18Sb(1), and 12Sb(2). Possible Zn interstitial sites in the interstitial model are indicated with light small circles. (b) The interstitial atoms have full occupancy and become ordered in the α phase (light blue circles). To help with comparison, only a part of a triclinic supercell is shown.

($\lambda=0.14248 \text{ \AA}$) for the 300 K data and 129.77 keV ($\lambda=0.095541 \text{ \AA}$) for the low-temperature measurements. Data were collected using the rapid acquisition PDF technique.¹⁸ Both neutron and x-ray data were processed to obtain the PDFs (Refs. 14 and 18) using programs PDFGETN (Ref. 19) and PDFGETX2,²⁰ respectively.

Three structural models based on the $R\bar{3}c$ framework and the α -phase superstructure were used for this study (Fig. 1): the mixed occupancy,¹³ vacancy,⁴ and interstitial² models. The α -phase superstructure, here named the α -structural model, accounts for superlattice peaks arising from ordered Zn interstitial defects below $T \approx 260 \text{ K}$.^{16,17} All the sites in the low-temperature α -structural model are fully occupied.

The structural modeling was carried out using the program PDFFIT2.²¹ Each model was taken as an initial structure, then lattice parameters, atomic coordinates, and isotropic displacement parameters (U_{iso}) were refined using a least-squares approach until the difference between the experimental and calculated PDFs was minimized. The atomic coordinates were constrained to retain the symmetry of the $R\bar{3}c$ space group for the mixed occupancy, vacancy, and interstitial models. For the α -structural model, the space group $C\bar{1}$ was used and the atomic coordinates were fixed to the values from the literature.¹⁶ For all the models, only two parameters were assigned for U_{iso} : one for Zn atoms and the other for Sb atoms regardless of different crystallographic sites. The refinement range was $1.5 < r < 20.0 \text{ \AA}$.

The PDF obtained from 15 K neutron data is shown in Fig. 2(a). The excellent signal-to-noise ratio of the data is evident from the negligibly small ripples on the base line of the PDF below 2 \AA compared to the PDF peaks. The first sharp peak at 2.7 \AA derives from the nearest-neighbor pairs of Zn–Zn, Zn–Sb, and Sb–Sb in the rhombohedral unit cell [Fig. 1(a)]. The calculated PDF from the refined α -structural model is plotted over the data with the difference shown in the curve below it. The refined values of the structural parameters are summarized in Table I. The model is in excellent agreement with the data without refinement of atomic coordinates, directly indicating that the local structure agrees well with the average structure in the α phase.

Now, we focus on the PDF of β -Zn₄Sb₃. The results of structural modeling on the neutron PDF at 300 K using the mixed occupancy, vacancy, and interstitial models are summarized in Table I. Reasonably good fits are obtained from each of the models with agreement factor, R_w ,²¹ of around 0.15 for mixed occupancy and vacancy models and lower for the interstitial model which has two to three times more refinable parameters. These fits are obtained at the expense of enlarged atomic displacement factors on the Zn sites, though the interstitial model does better in this regard. Enlarged atomic displacement factors may signify the presence of loosely coordinated “rattler ions”²² or alternatively nonthermal disorder that is not incorporated explicitly in the models.

The R_w^b values in Table I show how the results changed when U_{iso} was fixed to a smaller value of 0.01 \AA^2 , a value between the refined 15 and 300 K values and appropriate for a temperature in the vicinity of the structural phase transition, for both Zn and Sb atoms. Now, the insufficiency of each model emerges due to the sharpening of PDF peaks by

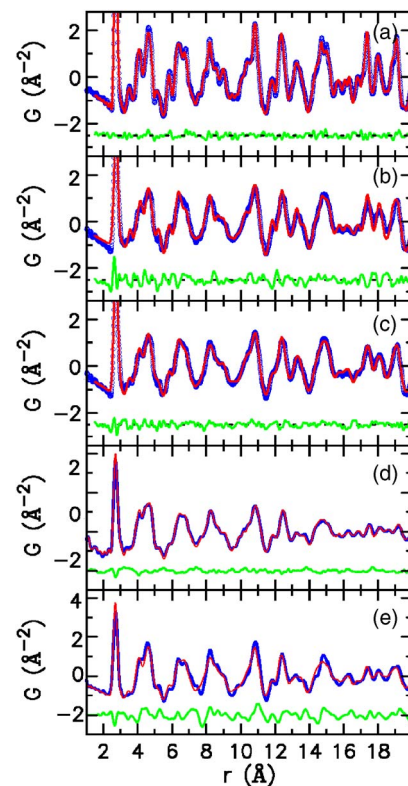


FIG. 2. (Color online) PDF refinement results and the change in PDF over α - β transition. (a) The experimental neutron PDF obtained at 15 K (blue circles) together with the calculated PDF from the refined α model (red line). (b) 300 K neutron data with the calculated PDF from the refined β -phase interstitial model. (c) The same data as (b) but this time the calculated PDF of the α -structural model. The PDFs in (b) and (c) were calculated with a fixed U_{iso} of 0.01 \AA^2 . In each case, the difference between the calculated and measured PDFs is plotted below the data. The good agreement in (c) indicates that the α -structural model explains the *local* structure of β -Zn₄Sb₃ with a smaller value of U_{iso} whereas the interstitial model does not (b). [(d) and (e)] Comparison of the change in PDF expected as the sample goes from the α to β phase. The PDF in the α phase is shown in light red line and the β phase in dark blue line. The difference is plotted below. (d) *Experimental* x-ray PDFs in β (270 K, dark blue line) and α (220 K, light red line) phases. (e) The *calculated* PDFs based on the average structures. U_{iso} used for the calculation is 0.01 \AA^2 for both interstitial and α -structural models. The observed changes in the local structure are much smaller than expected from the crystal structure models.

the small U_{iso} value. The case of the interstitial model is shown in Fig. 2(b). The results imply that the local structure of β -Zn₄Sb₃ is somehow more distorted than the three models suggest.

We also tried the α -structural model for the *local* structure of the 300 K data. It provides as good a fit as the other models did with just U_{iso} being refined. With fewer parameters, the resultant R_w value is comparable to the other models (Table I). The most interesting result was obtained when U_{iso} was fixed to 0.01 \AA^2 during the refinement [Fig. 2(c)]. Even though U_{iso} was fixed, a good fit was still obtained; the fluctuation in the difference curve is not significant and, most of all, the R_w value does not change much (Table I), implying

TABLE I. Refined structural parameters from various models. Lattice parameters and isotropic displacement parameters (U_{iso}) were refined for all models. The atomic coordinates (not reported here) were refined only for mixed occupancy, vacancy, and interstitial models being constrained to keep the $R\bar{3}c$ symmetry. The refinement range was $1.5 < r < 20.0$ Å.

	Mixed occupancy		Vacancy		Interstitial		α structural		
	Neutron (300 K)	X ray (300 K)	Neutron (300 K)	X ray (300 K)	Neutron (300 K)	X ray (300 K)	Neutron (300 K)	X ray (300 K)	Neutron (15 K)
a (Å)	12.2508(5)	12.231(2)	12.2444(5)	12.244(1)	12.2433(5)	12.234(2)	32.730(7)	32.576 (3)	32.553(5)
b (Å)							12.249(3)	12.220(6)	12.236(2)
c (Å)	12.432(1)	12.468(3)	12.430(1)	12.472(1)	12.427(1)	12.464(1)	10.896(3)	10.945(1)	10.872(2)
β							98.97(1)	99.25(1)	98.99(1)
Zn U_{iso} (Å ²)	0.0333(2)	0.0459(1)	0.0315(2)	0.0731(3)	0.0269(2)	0.0292(3)	0.0176(1)	0.0285(2)	0.0052(1)
Sb U_{iso} (Å ²)	0.01191(9)	0.0151(1)	0.0147(1)	0.0110(3)	0.0140(1)	0.0166(1)	0.0098(1)	0.0126(1)	0.00281(7)
n^a	9	9	9	9	18	18	6	6	6
R_w	0.153501	0.14236	0.150178	0.162943	0.110834	0.123122	0.116389	0.138129	0.083549
R_w^b	0.268002	0.242116	0.258401	0.291704	0.230391	0.227926	0.133564	0.159292	

^aNumber of parameters used.

^bResults with U_{iso} for both Zn and Sb atoms fixed to 0.01 Å².

that in the β phase the α -like structure is preserved locally. This result suggests that the enlarged U_{iso} on Zn sites in the β model is due to the averaging of different local environments in the cubic model and interstitials are not rattler ions.

As a further check of this hypothesis, we measured the temperature dependence of the local structure through the α - β phase transition at 260 K. Indeed, there is no significant change in the x-ray PDF on crossing the transition [Fig. 2(d)], compared to the expected change based on the α and β models [Fig. 2(e)], indicating that locally the structure is not changing even though there is a change in the average symmetry at this transition.

It is interesting to investigate what aspect of the α model makes it better for the low- r region of the PDF of β -Zn₄Sb₃ than the interstitial model even though they have similar numbers of Zn interstitial atoms. The improvement in fit is unlikely to be explained by the ordering arrangement of interstitial atoms in the α model since the defects themselves are only 10% in the fully occupied $R\bar{3}c$ framework^{2,16} and the consequent effect is small in the PDF. The reason seems to lie in the local coordination of the interstitial atoms in the respective models. The interstitial model provides possible Zn interstitial sites in a highly symmetric $R\bar{3}c$ structural frame [Fig. 1(a)] but not their influence of relaxing the positions of neighboring atoms. Accordingly, large U_{iso} values are necessary for the interstitial model to get sufficiently broad PDF peaks. However, the lower-symmetry atomic arrangement in the α model [Fig. 1(b)] correctly captures the perturbed environment of the interstitial atoms. Since the local structure does not change at the α - β -phase transition, the Zn interstitial defects persist but lose their long-range order forming the α -like domains in the β phase.

When point defects are discovered in a material, particularly charged point defects that require other charge balancing defects, one should expect local structural distortions or rearrangements that will lead either to long-range order and a superstructure or to short-range-ordered nanometer size do-

main that are not detected with traditional diffraction techniques. In the Zn₄Sb₃ case, the Zn interstitials order at low temperature, resulting in a new crystallographic phase and a superstructure in the diffraction pattern.^{16,17} This tendency to order locally will reduce Coulombic and elastic strain energies. At high temperature, the defects prefer to disorder to increase the entropy, but the strong tendency toward local ordering persists, resulting in nanoscale domains, or short-range order with a finite coherence length, such as was found here.

In the β phase, the local α -like domains must be oriented

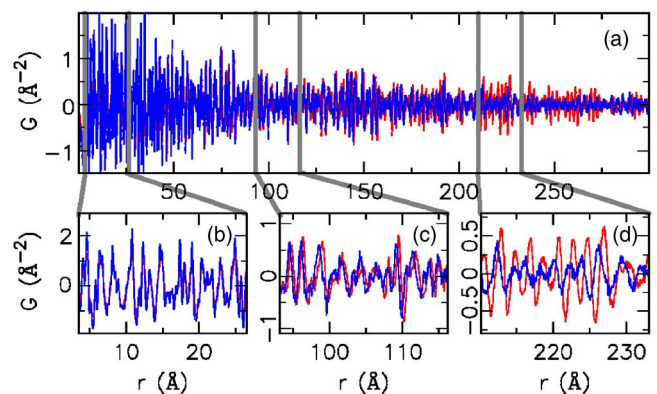


FIG. 3. (Color online) Comparison of 15 and 300 K PDFs in different r regions. (a) Comparison of low- (15 K, dark blue line) and high-temperature (300 K, light red line) neutron PDFs of Zn₄Sb₃ plotted over a wide range of r to 300 Å. (b)–(d) are the same data but plotted on expanded r scales. Note that at low r , the 300 K PDF has broader and lower peaks, but at high r the situation is reversed. PDF peaks broaden with temperature due to increased thermal motion as evident at low r (b). The PDF peaks are sharper and higher at room temperature in the high- r region (d) because the 300 K data are from the high-symmetry β phase. A rough estimate of the size of the local α domains can be obtained from where the behavior switches over (c).

in such a way that crystallographically the interstitial atoms appear in a randomly distributed way over three possible interstitial sites in the average $R\bar{3}c$ structure. However, the similarity of the local structure suggests that locally the interstitial atoms avoid each other in the β phase, resulting in short-range defect ordering that resembles the α phase. The rhombohedral β structure is incomplete as a local structure as it has atomic distances that are unphysically short. This work confirms that the actual local structure contains reasonable atomic distances (such as those in the α phase with no indication of a Zn–Zn bond⁵) and that nanoscale domains must exist. We would like to estimate the domain size, or coherence length, of this local order. At low r , the PDF is probing below this domain length scale and finds an α -like local structure; however, the PDF at high r (consistent with the average x-ray-diffraction measurements²) averages over a longer length scale and results in the different average structure of β -Zn₄Sb₃. A striking feature found in a comparison of the 300 and 15 K neutron PDFs is an inversion of the relative PDF peak heights in the region between 60 and 120 Å (Fig. 3). Below 60 Å, the PDF peaks in the 15 K data are taller than those in the 300 K data [Fig. 3(b)], as expected due to the reduced thermal motion. However, above 120 Å, the opposite is observed [Fig. 3(d)]. If there is no phase change, the PDF peaks will broaden with increasing temperature at all distances r , but this is not observed. The anomalous T dependence is explained due to the fact that at higher r the PDF reflects the higher symmetry of the β struc-

ture and higher symmetry results in sharper PDF peaks. The fact that the low- r peaks broaden with increasing temperature and do not sharpen at the phase transition is a strong evidence that the local symmetry is lower than the average symmetry. We can roughly estimate the diameter of the lower-symmetry domains from the crossover in peak-broadening behavior. The crossover happens in the region of 60–120 Å [Fig. 3(c)]. We therefore estimate the α -domain size to be of the order of, but probably somewhat less than, 10 nm, where the effects on the PDF of the higher average symmetry start to dominate. A more thorough study is necessary to estimate the exact domain size.

We have investigated the local structure of Zn₄Sb₃ using the PDF technique. The result shows that the structure of β -Zn₄Sb₃ at 300 K is composed of nanoscaled α -like domains. Like other recently developed high ZT thermoelectric materials, the exceptionally low thermal conductivity of β -Zn₄Sb₃ may be attributed to these nanoscale structural domains.

The authors gratefully acknowledge F. Gascoin, Th. Proffen, D. Robinson, D. Wermeille, X. Qiu, and A. Masadeh for experimental help and S. D. Mahanti for useful discussions. This work was supported by the NSF through Grant No. DMR-0304391. The Lujan Center, APS, and the MUCAT sector at APS are funded by DOE through Contract Nos. W-7405-ENG-36, W-31-109-ENG-38, and W-7405-ENG-82, respectively.

*Electronic address: billinge@pa.msu.edu

¹F. J. DiSalvo, *Science* **285**, 703 (1999).

²G. J. Snyder, M. Christensen, E. Nishibori, T. Caillat, and B. B. Iversen, *Nat. Mater.* **3**, 458 (2004).

³G. A. Slack, in *CRC Handbook of Thermoelectrics*, edited by D. M. Rowe (CRC, Boca Raton, FL, 1995), Chap. 34.

⁴Y. Mozharivskyj, A. O. Pecharsky, S. Bud'ko, and G. J. Miller, *Chem. Mater.* **16**, 1580 (2004).

⁵F. Cargnoni, E. Nishibori, P. Rabiller, L. Bertini, G. J. Snyder, M. Christensen, C. Gatti, and B. B. Iversen, *Chem.-Eur. J.* **10**, 3862 (2004).

⁶S. Bhattacharya, R. P. Hermann, V. Keppens, T. M. Tritt, and G. J. Snyder, *Phys. Rev. B* **74**, 134108 (2006).

⁷W. Kim, J. Zide, A. Gossard, D. Klenov, S. Stemmer, A. Shakouri, and A. Majumdar, *Phys. Rev. Lett.* **96**, 045901 (2006).

⁸K. F. Hsu, S. Loo, F. Guo, W. Chen, J. S. Dyck, C. Uher, T. Hogan, E. K. Polychroniadis, and M. G. Kanatzidis, *Science* **303**, 818 (2004).

⁹H. Lin, E. S. Božin, S. J. L. Billinge, E. Quarez, and M. G. Kanatzidis, *Phys. Rev. B* **72**, 174113 (2005).

¹⁰J. Androulakis, K. F. Hsu, R. Pcionek, H. Kong, C. Uhr, J. J. D'Angelo, A. Downey, T. Hogan, and M. G. Kanatzidis, *Adv. Mater. (Weinheim, Ger.)* **18**, 1170 (2006).

¹¹L. D. Hicks and M. S. Dresselhaus, *Phys. Rev. B* **47**, 12727

(1993).

¹²R. Venkatasubramanian, E. Siivola, T. Colpitts, and B. O'Quinn, *Nature (London)* **413**, 597 (2001).

¹³H. W. Mayer, I. Mikhail, and K. Schubert, *J. Less-Common Met.* **59**, 43 (1978).

¹⁴T. Egami and S. J. L. Billinge, *Underneath the Bragg Peaks: Structural Analysis of Complex Materials* (Pergamon, England, 2003).

¹⁵S. J. L. Billinge and M. G. Kanatzidis, *Chem. Commun. (Cambridge)* **2004** (7), 749.

¹⁶J. Nylén, M. Andersson, S. Lidin, and U. Häussermann, *J. Am. Chem. Soc.* **126**, 16306 (2004).

¹⁷A. S. Mikhaylushkin, J. Nylén, and U. Häussermann, *Chem.-Eur. J.* **11**, 4912 (2005).

¹⁸P. J. Chupas, X. Qiu, J. C. Hanson, P. L. Lee, C. P. Grey, and S. J. L. Billinge, *J. Appl. Crystallogr.* **36**, 1342 (2003).

¹⁹P. F. Peterson, M. Gutmann, T. Proffen, and S. J. L. Billinge, *J. Appl. Crystallogr.* **33**, 1192 (2000).

²⁰X. Qiu, J. W. Thompson, and S. J. L. Billinge, *J. Appl. Crystallogr.* **37**, 678 (2004).

²¹T. Proffen and S. J. L. Billinge, *J. Appl. Crystallogr.* **32**, 572 (1999).

²²B. C. Sales, B. Chakoumakos, D. Mandrus, and J. W. Sharp, *J. Solid State Chem.* **146**, 528 (1999).